Projectile rapidity pions in 775 MeV/nucleon ^{139}La + ^{12}C and ^{139}La + ^{139}La reactions

O. Hashimoto, H. Hamagaki, T. Kobayashi,* K. Nakayama,† Y. Shida, I. Tanihata,* O. Yamakawa‡, and N. Yoshikawa
Institute for Nuclear Study, University of Tokyo, Tanashi, Tokyo 188, Japan

S. Nagamiya
Department of Physics, Columbia University, New York, New York 10027

J. A. Bistirlich,§ K. M. Crowe, T. J. Humanic,‖ M. Justice, J. O. Rasmussen, and Y-W. Xu¶
Lawrence Berkeley Laboratory, University of California, Berkeley, California 94720
(Received 9 August 1993)

Negative pion spectra emitted in the reactions of 775 MeV/nucleon ^{139}La + ^{12}C and ^{139}La + ^{139}La reactions have been measured in coincidence with the projectile fragments using the HISS spectrometer at the Bevalac. Prominent peaks near the beam velocity were observed in the pion spectra. Position and widths of the peaks were studied as a function of the "sum charge" of projectile fragments, which is a good measure of impact parameter; the smaller the "sum charge," the smaller the impact parameter. The peak position down shifts with the smaller "sum charge." The pion peak is wider in the transverse than in the longitudinal direction, possibly mirroring the velocity dispersions of projectile fragments in the early stage of reactions.

PACS number(s): 25.75.+r, 25.70.Mn

I. INTRODUCTION

High-energy heavy-ion collisions in the 1 GeV/nucleon energy region have been the field of intensive study in past years. Many basic features of the collisions are explained by spectator-participant models. In this energy range, pions are abundantly produced in the participant region and generally show a characteristic exponential distribution in momentum. In the low p_T region, however, pion spectra behave differently. Benenson *et al.* [1] first observed a peak near the beam rapidity in zero-degree spectra of negative pions in Ne + NaF reactions at nominal beam energies from 125 to 400 MeV/nucleon. The effect was attributed to Coulomb interactions between a pion and the projectile fragment. Sullivan *et al.* [2] subsequently studied double-differential cross sections of negative and positive pions at forward angles in Ne and Ar induced reactions in the beam energy region between 280 and 535 MeV/nucleon. Lebrun *et al.* also studied the Coulomb-enhanced peak in a ^{16}O induced reaction at incident energies lower than 93 MeV/nucleon [3]. Bertsch *et al.* [4], Koonin *et al.* [5], Gyulassy *et al.* [6], and Radi *et al.* [7] theoretically investigated the strong Coulomb effects on charged-pion spectra in heavy-ion reactions at the Bevalac energies. Pions near the beam rapidity are expected to be sensitive to the projectile-fragment charge and its momentum distributions, because Coulomb interactions between the projectile fragments and the pions produced in the participant region distort the pion spectra. By observing the small-angle pion spectrum near the beam rapidity in coincidence with projectile fragments, particularly with high-Z projectiles, it is hoped that more will be learned about dynamics of high-energy heavy-ion collisions including Coulomb interactions in the 1 GeV/nucleon region. The present paper reports on the first coincidence measurement of projectile fragments and negative pions in heavy-ion induced reactions.

II. EXPERIMENTS

A ^{139}La beam of 802 MeV/nucleon was accelerated and extracted from the Bevalac of the Lawrence Berkeley Laboratory. The slowly extracted beam was transported to an experimental area where the superconducting spectrometer HISS [8] was installed. A typical beam intensity was 10^5 particles/spill with the spill duration of 1 sec and the spill interval of 5 sec. The energy incident on the target was calculated to be 775 MeV/nucleon (rapidity = 1.21) after taking into account the energy loss by materials along the beam line, such as windows of vacuum pipes,

*RIKEN, 2-1 Hirosawa, Wako-shi, Saitama 351-01 Japan.
†Toshiba Corporation, Energy Science & Technology Laboratory, Research & Development Center, Kawasaki, Kanagawa 210 Japan.
‡Fukui Prefectural College, Ouhata, Fukui 910 Japan.
§SSC Laboratory, 2550 Beckleymeade Ave., MS 1002, Dallas, TX 75237-3946
‖Department of Physics, The Ohio State University, 174 W. 18th Ave., Columbus, OH 43210.
¶No.21 Cui WaiLu, Hai Dian District, Beijing, China.

beam profile monitors, a scintillation counter in the beam line, etc. The average energy of the La beam at target center is estimated to be 752 MeV/nucleon (rapidity = 1.19) for the carbon target and 759 MeV/nucleon (rapidity = 1.20) for the lanthanum target, respectively, considering the thickness of the target was 0.901 g/cm^2 for carbon and 0.964 g/cm^2 for lanthanum. The experimental setup consists of three components as illustrated in Fig. 1: (1) Beam detectors, (2) negative pion detectors, and (3) projectile fragment detectors (see Table I). The experiment utilized the HISS magnet and its time-of-flight wall T4-1 and -2 for detecting the projectile fragments. A large magnetic volume of the HISS magnet was used for the momentum analysis of both projectile fragments and forward-emitted pions near the projectile rapidity. The beam detectors, negative pion detectors, and an additional smaller time-of-flight wall for fragment detection were added to the original HISS detector configuration for the present experiment. The target was located 1.05 m upstream from the center of the HISS dipole magnet, so that the pion arm formed a nearly radial focusing 180° spectrometer (see Table II).

Beam particles were measured individually by a thin scintillator, T0, and a wire chamber, WC0. The scintillator was 10 cm × 10 cm with the thickness of 0.254 mm and had a long light guide to avoid the effect of the HISS magnet fringing field. The T0 scintillator generated a time-zero signal together with its pulse height. Beam particles were identified by measuring their energy loss in the scintillator. The pulse-height information was also used to reject pile-up events within a 100 nsec time window, since the pulse heights were significantly larger for pile-up events than for beam particles. The wire chamber WC0 consisted of three planes and served to record the position of the beam at the target.

Negative pions were deflected by almost 180°, and the trajectories were measured by wire chambers, WC1 and WC2. Two sets of scintillator walls, T1 and T2, and a water-Cherenkov-counter wall, were installed, as seen in Fig. 1. The chamber WC1 was 30-cm high and 65-cm wide and consisted of X, Y, and Z planes in which the spacing of anode wires were all 3-mm. The WC2, 40-cm high and 75-cm wide, was located near the approximate focal plane of the pion arm. It consisted of four planes

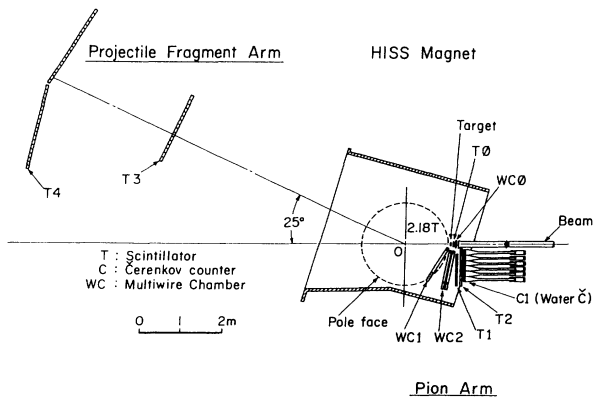

FIG. 1. Schematic drawing of the experimental setup.

TABLE I. Detectors used in the present experiment. T stands for a scintillator, and WC for a wire chamber.

	Beam Detectors
T0	10 cm × 10 cm × 0.254 mm
WC0	12 cm × 12 cm
	X(2 mm), Y(2 mm), Z(3 mm)
	Negative pion detectors
WC1	30 cm × 65 cm
	X(3 mm), Y(3 mm), Z(3 mm)
WC2	40 cm × 75 cm
	$X1$(3 mm), U(6 mm), V(6 mm), $X2$(3 mm)
T1	40 cm × 100 cm × 0.5 cm
T2	50 cm × 100 cm × 0.5 cm
	Projectile fragment detectors
T3	90 cm × 160 cm × 0.5 cm
T4-1	250 cm × 300 cm × 2.5 cm
T4-2	250 cm × 300 cm × 2.5 cm

$X1$, U, V, and $X2$. The scintillator wall, T1, was segmented into 5 vertical slats, T2 into 6, and the Cherenkov wall into 6. The water Cherenkov counter was used to reject electron contamination in the pion spectra.

The projectile fragment arm was equipped with two scintillator walls, T3 and T4. The T3 was 1.6-m wide and was segmented into 16 pieces, each of which was 90-cm high, 10-cm wide, and 0.5-cm thick. The T4 consisted of two walls which were 2.5-m high and 2-m wide. Each wall was divided into scintillator bars 2.5-m high, 10-cm wide, and 2.54-cm thick. At both ends of each scintillator paddle were mounted 5 cm phototubes. The projectile-fragment arm detected projectile fragments emitted at forward angles and measured time-of-flight and pulse height. The pulse heights of T3 and T4 gave information on the charge of a particle passing through the scintillator. The pulse-height-to-charge relation was calibrated with the use of ^{40}Ar and ^{139}La beams. Beam particles and associated projectile fragments were swept by the HISS magnet over all the scintillator slats. The T3 scintillator wall was able to resolve individual charges of the projectile fragments up to charge 18. Due to the saturation effect of a scintillator, the pulse height is not proportional to Z^2 for high Z. The charge was fitted to the experimental data by a third-order polynomial. The uncertainty of the fragment charge determined by the pulse height of T3 and T4 was estimated to be less than 1 for a charge smaller than 20, and less than 1.5 for charges up to 60.

Events were triggered when a particle hit two scintillators, T1 and T2. Data from the projectile fragment arm

TABLE II. Summary of experimental parameters.

Beam	^{139}La
Beam intensity	$\sim 10^5$ particles/spill
Beam energy at the target	775 MeV/nucleon
Target and thickness	^{12}C 0.901 g/cm^2
	^{139}La 0.964 g/cm^2

and the beam detectors were recorded for those triggered events. Target-out runs showed the background was less than 1% of the total spectrum.

The acceptance of the pion arm was calculated by generating simulated events from the target position uniformly in transverse and longitudinal momentum space. The Monte Carlo events were generated using the full three-dimensional field map of the HISS magnet which was measured by the HISS group of LBL. The pion-arm acceptance well encompasses the beam-velocity peak at forward angles. Hit positions at the wire chambers and scintillators were also recorded to be used for further analysis.

The projectile fragment arm detected projectile fragments with $Z/A \leq 1/2$ emitted at forward angles. Most protons were deflected beyond this arm. Only the forward-going trajectories were selected by requiring a coincidence between the two walls (TA3 and TA4), which were segmented as described above.

III. ANALYSIS

The data were analyzed to derive pion momenta around the beam rapidity, projectile fragment charges, and fragment "sum charge."

The analysis procedure to obtain the pion momentum was as follows. First, pion trajectories were generated by solving the equations of motion through the magnet with use of the full three-dimensional field map. Hit positions at all the wire chamber planes and scintillators of the pion arm were recorded and used for fitting the pion momentum as a function of chamber hit positions. The program ERIKA [9] was employed to evaluate coefficients of the Chebychev polynomials which calculate the pion momentum, hit positions at WC1, T1, and T2 as a function of those at WC0 and WC2.

Secondly, the hit position at the target was determined by the WC0 data. Good tracks that fired all four planes of WC2, which is located near the focal plane of the pion arm, were then selected. Using the hit positions at WC0 and WC2, the interpolated and extrapolated crossing positions at WC1, T1, and T2 were calculated based on the Chebychev polynomial, and consistency of hit positions at WC1, T1, and T2 was examined. Momentum of the particle was calculated for those events which gave correct hit positions at WC1, T1, and T2. Using the time-of-flight information and the momentum, the mass of the particle was derived. The momentum and angular resolutions are estimated to be $\delta p_{\rm rms} = 1.1$ MeV/c and $\delta\theta_{\rm rms} = 0.01$ rad, respectively.

The fragment charge was determined by analyzing the pulse height of the scintillators T3 and T4, which measured projectile fragments. These scintillators gave not only the pulse height information, but also the hit position of the fragment. The consistency of the hit position, both in x and y coordinates, and charge at T3 and T4 was examined, and the proper track was selected. For multiple fragment events, all charges were added up to obtain the "sum charge."

The projectile fragment arm did not cover beam-rapidity protons whose rigidity is smaller. Charged particles with $Z \geq 2$ were analyzed as projectile fragments. The measured "sum charge" of the projectile fragments is, therefore, smaller than the true one.

The charge resolution of the "sum charge" around $Z = 57$ was evaluated from the shape of maximum edge for the sum charge spectrum and was estimated to be about $\Delta Z = 5$. A larger error in Z, as compared to the detector resolution, is thought due to the loss of the detection of protons.

The absolute value of the cross section was extracted after evaluating the number of beam particles on the target, the chamber efficiency, the tracking efficiency, the pion decay-in-flight correction, and the geometrical acceptance.

The number of beam particles at the target was directly measured by the T0 scintillator, and correction for pile-up events was also applied. The reconstruction and analysis efficiency of the beam counters was about 0.82. The efficiency of wire chambers WC1 and WC2 in the present analysis was 97% and 88%, respectively. In the case of WC2, the firing of all four planes was required in the analysis, as previously described. The survival rate of pions in flight was estimated to be 0.84 ± 0.03 from the Monte Carlo calculation. Because of the semi-isochronous optics of the pion arm, the decay-in-flight correction for pions turned out to be constant to the first order in the pion momentum range from 80 to 300 MeV/c. The geometrical acceptance was determined by tracking the trajectories in the HISS magnet as already described. Taking into account these correction factors, invariant cross sections were obtained as a function of

TABLE III. Pion-peak fit parameters (La + C reaction).

$Z_{\rm sum}$[a]	$y_{\rm peak}$	W_y	$W_\perp$ ($m_\pi c$)	$d\sigma_{\rm peak}$ (mb/MeV^2)	$\chi^2/N_{\rm DF}$	Integrated $\sigma_{\rm peak}$(mb)
50–60	1.2077 ± 0.0049	0.060 ± 0.008	0.072 ± 0.008	0.0036 ± 0.0006	1.06	0.12 ± 0.04
40–50	1.1983 ± 0.0032	0.049 ± 0.006	0.077 ± 0.010	0.0054 ± 0.0008	1.07	0.17 ± 0.06
30–40	1.1920 ± 0.0025	0.059 ± 0.005	0.068 ± 0.004	0.0114 ± 0.0009	0.94	0.33 ± 0.06
20–30	1.1854 ± 0.0014	0.043 ± 0.003	0.066 ± 0.003	0.0222 ± 0.0015	1.27	0.45 ± 0.09
10–20	1.1739 ± 0.0020	0.059 ± 0.002	0.070 ± 0.003	0.0181 ± 0.0011	1.17	0.57 ± 0.07
5–10	1.1957 ± 0.0043	0.050 ± 0.008	0.085 ± 0.016	0.0031 ± 0.0007	1.11	0.12 ± 0.06
inclusive	1.1864 ± 0.0011	0.054 ± 0.002	0.068 ± 0.002	0.0789 ± 0.0032	1.23	2.10 ± 0.17

[a] 50–60 means $50 < Z_{\rm sum} \leq 60$.

TABLE IV. Pion-peak fit parameters (La + La reaction).

Z_{sum}[a]	y_{peak}	W_y	$W_\perp$ ($m_\pi c$)	$d\sigma_{peak}$ (mb/MeV^2)	χ^2/N_{DF}	Integrated σ_{peak}(mb)
50–60	1.2205 ± 0.0097	0.040 ± 0.014	0.081 ± 0.022	0.0086 ± 0.0028	1.36	0.25 ± 0.18
40–50	1.2013 ± 0.0039	0.041 ± 0.005	0.088 ± 0.018	0.0145 ± 0.0033	1.40	0.49 ± 0.24
30–40	1.2026 ± 0.0056	0.070 ± 0.013	0.077 ± 0.012	0.0240 ± 0.0049	0.70	1.07 ± 0.41
20–30	1.1976 ± 0.0025	0.059 ± 0.005	0.091 ± 0.008	0.0447 ± 0.0040	1.13	2.37 ± 0.50
10–20	1.1996 ± 0.0021	0.050 ± 0.004	0.099 ± 0.010	0.0517 ± 0.0049	0.89	2.76 ± 0.64
5–10	1.1895 ± 0.0058	0.056 ± 0.008	0.130 ± 0.045	0.0143 ± 0.0030	1.34	1.47 ± 1.08
inclusive	1.1993 ± 0.0017	0.057 ± 0.003	0.105 ± 0.009	0.1694 ± 0.0114	0.87	11.51 ± 2.18

[a] 50–60 means $50 < Z_{sum} \leq 60$.

rapidity and transverse momentum. Errors of cross sections include statistical and the estimated 20% systematic errors. It is noted that the present cross section is consistent with the one extrapolated to $p_T = 0$ in the data reported by Hayashi *et al.* [10] They measured the angular distribution and the momentum distribution for pions in La + La reaction at 800 MeV/nucleon with a magnetic spectrometer.

IV. RESULTS AND DISCUSSION

The experimental cross sections of pion-inclusive spectra, as well as coincidence spectra with the fragment "sum charge," were tabulated in Tables III and IV in the form of invariant cross sections (mb/MeV^2) for the longitudinal-momentum region $80 \leq p_L \leq 240$ MeV/c and for the transverse-momentum region of $0 \leq p_T \leq 40$ MeV/c. For the coincidence data, the fragment "sum charge" was binned in $\Delta Z = 10$ (or 5 for $Z = 5$–10). A two-dimensional spectrum was fitted by a single two-dimensional Gaussian function on a flat background. For each "sum charge" the primary data were binned by laboratory-frame longitudinal and transverse momenta. However, they were converted to rapidity and $p_T/m_\pi c$ bins to facilitate interpretation. The nonlinear, least square-fitting program MINUIT from the CERN library was used for the actual fitting. The following seven parameters were left adjustable: peak height, the rapidity at peak center, the width in rapidity, the width in transverse momentum ($p_T/m_\pi c$), and 3 parameters for the linear background. Fits were made for each data set in the bins of either 5 or 10 in the fragment sum charge up to $Z_{sum} = 60$. The fitted parameters, as well as integrated peak cross sections, are tabulated in Tables III and IV. It is emphasized that the present data unambiguously demonstrate that the pion peak is formed by Coulomb interactions between projectile fragments and pions through observing correlation between projectile fragment charges and pion spectra at 0°.

A. Pion inclusive spectra

In Fig. 2 are shown the singles spectra of pions emitted at forward angles with $p_T \leq 10$ MeV/c as a function of rapidity both for the La + C and La + La reactions. It is evident from the figure that the π^- cross section has a maximum around the beam rapidity at forward angles for both reactions. These peaks are much enhanced compared to the case of lighter projectiles reported previously [1,2]. The La + C reaction gives much more distinct peak structure than the La + La reaction.

Because of energy losses of the beam particle and the pion in the target, rapidity distribution of the observed pions can be shifted and broadened even if pions are created at the rapidity of beam particles. For the present target thickness and the beam energy at the entrance to the target, the rapidity distribution of detected pions that correspond to the beam rapidity pions at reaction

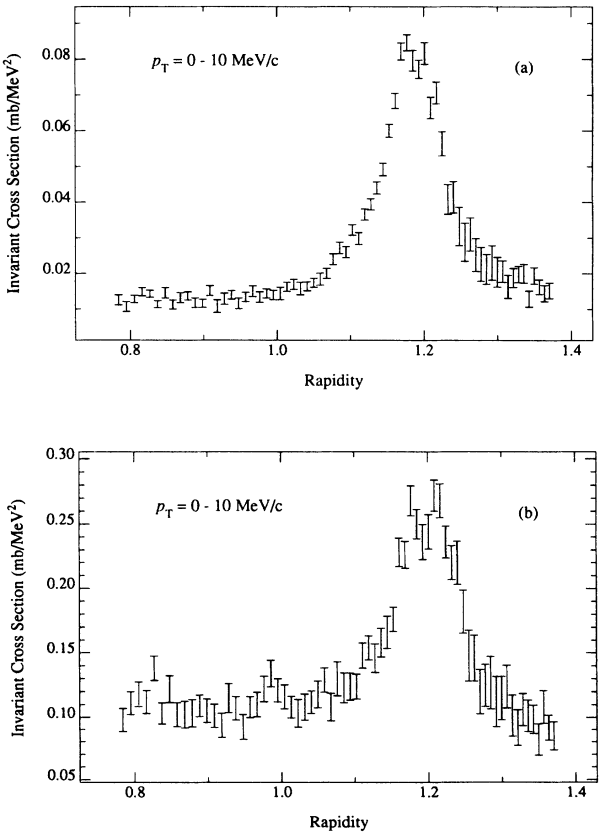

FIG. 2. Singles rapidity spectra of forward-emitted pions as a function of rapidity for transverse momentum less than 10 MeV/c. (a) La + C reaction, (b) La + La reaction.

points will range from $y_\pi = 1.201$ to 1.177 for the La + C reaction and $y_\pi = 1.204$ to 1.187 for the La + La reaction. The observed pion spectrum should be, therefore, the one convoluted uniformly over this rapidity range. As seen in Fig. 2, the peak position for the lanthanum target lies at a rapidity slightly higher than that for the carbon target. This difference can be accounted for by the difference of the ranges for the La beam in the La and C targets.

In Fig. 3 are shown pion cross sections as a function of rapidity for transverse momenta from 2 to 4 MeV/c both for La + C and La + La reactions. No "sum charge" selections were applied here.

Transverse momentum dependence of the cross section at the peak position ($1.165 \leq y \leq 1.205$ for La + C and $1.181 \leq y \leq 1.221$ for La + La) are shown in Fig. 4. Again, no cuts on "sum charge" were taken for this figure. Solid curves both in Figs. 3 and 4 are the fitted result for the data near the peaks by the two-dimensional Gaussian.

B. Fragment "sum charge"

In the participant-spectator model, the projectile fragments originate from that part of the projectile nucleus not overlapping the target nucleus. The projectile fragments could have a mean velocity slightly less than that of the beam with a dispersion in longitudinal and transverse momenta. Brady *et al.* [11] earlier studied ^{139}La fragmentation at the Bevalac, and we shall refer to their results again later. The projectile-fragment arm of the present experiment well covers the cone of the fragments. The measured "sum charge" will be, therefore, a better measure of the impact parameter. Recently, a GSI group measured this correlation for various targets [12].

In Fig. 5 are shown the pion peak cross sections as a function of the "sum charge" for the La + C and La + La reactions. The peak cross section shows a maximum at the sum charge of 10–20. This is due to the compensation of two mechanisms. One is that the pion production rate itself decreases as the impact parameter increases (or, the sum charge increases). The other, however, is that the production cross section of projectile fragments decreases as the impact parameter decreases. Since the peak cross section of pion production is associated with the projectile fragment, this cross section would decrease as the production rate of projectile fragment decreases. A slightly different shape of the peak cross section between La + C and La + La is observed. It will be interesting to study this feature theoretically in the future.

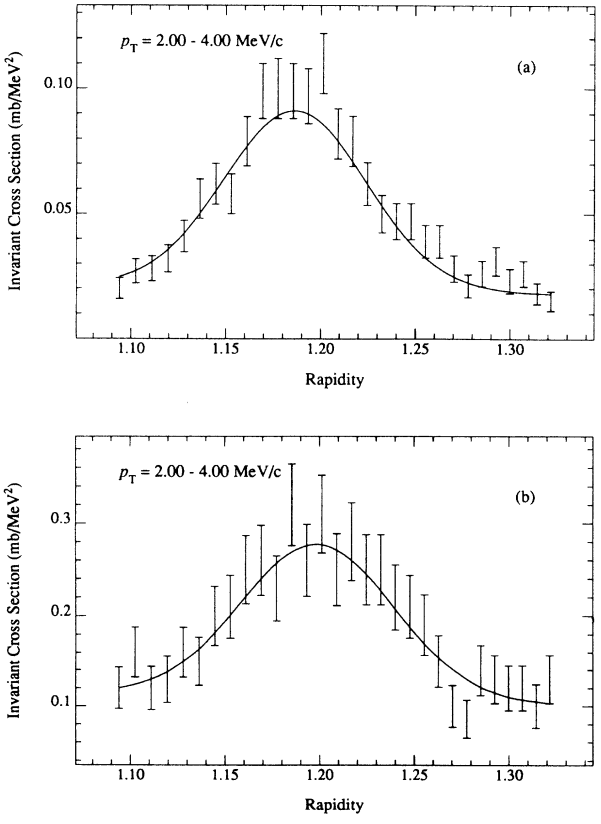

FIG. 3. Inclusive spectra of pion rapidity with transverse momentum 2 MeV $\leq p_T \leq$ 4 MeV. (a) La + C reaction, (b) La + La reaction. The solid curve is obtained by fitting the spectra with a single two-dimensional Gaussian and a flat background for the two-dimensional data.

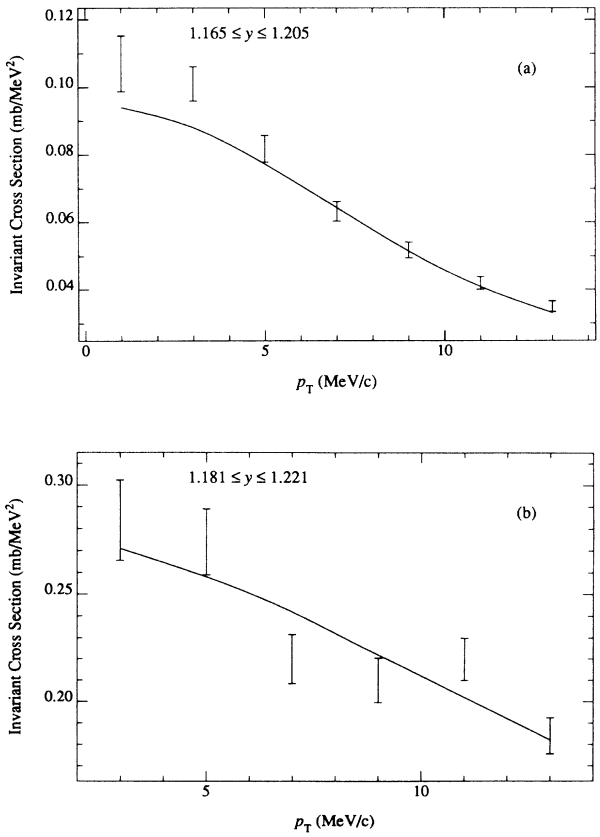

FIG. 4. Inclusive spectra of pion transverse momentum at the peak rapidity. (a) La + C reaction, (b) La + La reaction. The solid curve is obtained by fitting the spectra with a single two-dimensional Gaussian and a flat background.

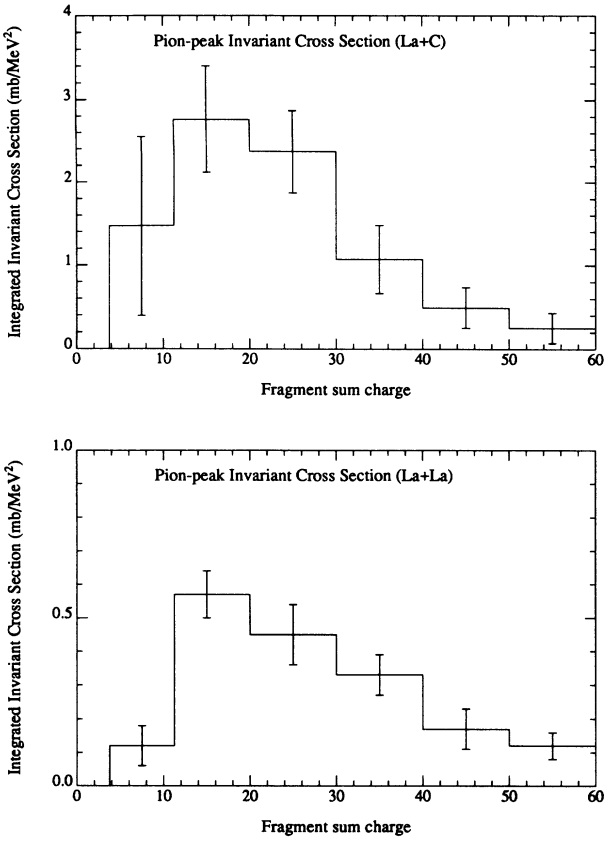

FIG. 5. Pion peak cross section from the two-dimensional Gaussian fit as a function of "sum charge" for La + C (open circle) and La + La (closed circle) reactions.

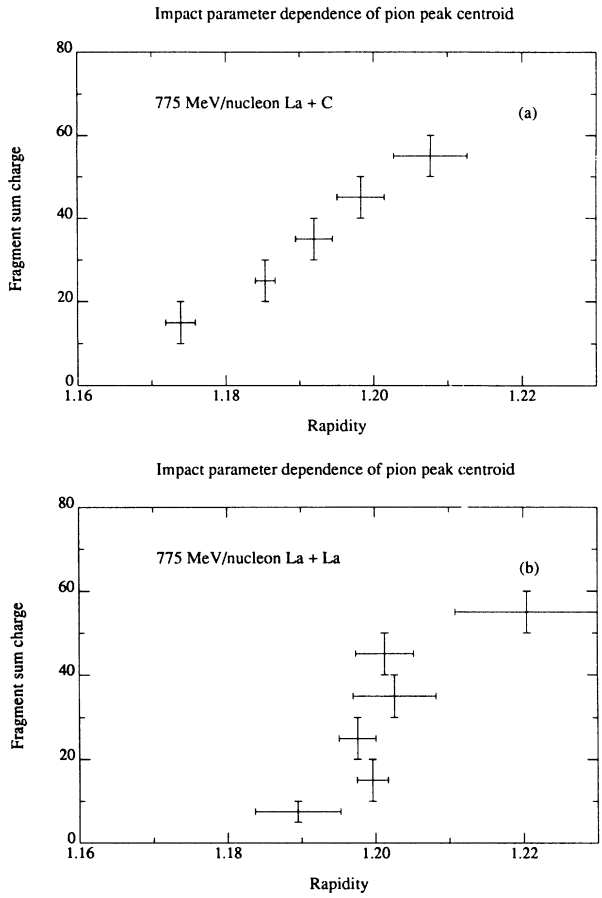

FIG. 6. Rapidity of the pion peak as a function of fragment "sum charge." The two-dimensional Gaussian fitting was performed in the peak region with constant background. (a) La + C reaction, (b) La + La reaction.

C. Peak position

The peak position around the beam velocity is plotted against the "sum charge" in Fig. 6 for the La + C and La + La reactions. It is shown in Fig. 6(a) that the pion peak position depends on the projectile "sum charge" in the case of the La + C reaction. The greater down shifts of the peak position go with the smaller fragment "sum charge," or with the smaller impact parameter. The peak positions in the La + La reaction show less distinct dependence on the "sum charge." It is noted that the spread of the pion rapidity due to the energy losses of the beam and emitted pion is much smaller than the width of the peak, and therefore peak position of the spectrum can be well defined.

Since the forward emitted pions probe the velocity and its dispersion of the projectile fragments through Coulomb interactions, it is naively expected that the downshift is due to the participant-spectator interaction that decelerates the velocity of projectile fragments.

If the downshift of the pion peak momentum is due to that of the projectile fragment, the pion momentum shift can be expressed as

$$\Delta p_\pi = (\Delta p_A / A_{\mathrm{frag}})(m_\pi / m_N), \quad (1)$$

where $\Delta p_A / A_{\mathrm{frag}}$ represents the lost momentum per nucleon for the projectile fragment, and m_π and m_N the masses of a pion and nucleon. The downshift of the projectile fragment momentum can be expressed as proportional to the number of nucleons in the participant region, $\Delta p_A = \alpha A(b)$, where $A(b)$ is number of nucleons in the participant region. Further assuming that the charge in the projectile fragment region is roughly proportional to its mass, the downshift of the pion momentum will be written as

$$\Delta p_\pi = [\alpha Z(b)/Z_{\mathrm{frag}}](m_\pi / m_N), \quad (2)$$

where $Z(b)$, the charge in the participant region with impact parameter b, can be calculated as lost charge $Z(b) = Z_{\mathrm{proj}} - Z_{\mathrm{frag}}$. $Z_{\mathrm{frag}} \approx Z_{\mathrm{sum}}$ is assumed, while it will be underestimated as described earlier. The "friction" coefficient α is then estimated to be ≈ 15 MeV/c by fitting the La + C data. The projectile fragments will be decelerated by 15 MeV/c nucleon per participant nucleon on the average. The La + La data gives a much smaller value of $\alpha \sim 2.5$ MeV/c nucleon.

In the present discussion, it is implicitly assumed that the pion-peak rapidity in the very peripheral collisions, or those with the largest "sum charge," be the same with that of the beam rapidity. However, the pion peak rapidities slightly exceed the beam rapidity for the highest sum-charge bins. The origin of the discrepancy is possi-

bly due to a systematic error in the measured absolute momenta by 2–3 %, which can explain the above discrepancy.

D. Peak widths

Observed Gaussian widths are plotted as a function of the "sum charge" in Figs. 7 and 8. The widths in the longitudinal direction are plotted in the unit of rapidity, while those in the transverse direction in the unit of $p_T/(m_\pi)c$ for both La + C and La + La reactions. It is noted that rapidity and $p_T/(m_\pi)c$ are kinematical quantities that can be compared to each other as longitudinal and transverse "velocities," since the ranges of interest for these quantities are nonrelativistic when viewed from a frame that corresponds to a center of the pion peak.

Two features are observed: (a) The widths are fairly constant over the "sum charge," and (b) the widths in transverse direction are larger than that in the longitudinal direction, showing an oblate shape in the projectile frame. Radi *et al.* [7] pointed out that the pion peak tracks the projectile fragment velocity and attributed most of the peak width to the velocity dispersion of the fragment in the projectile frame. In this picture, the oblate distribution implies that the velocity dispersion of fragments in the perpendicular direction is broader than that in the longitudinal. This observation can possibly be tied in with that of Brady *et al.* in a 1.2 GeV/nucleon ^{139}La + C reaction [11]. They reported that the p_T dispersions for lanthanum spectator fragments significantly exceed those predicted by models that assume random sudden removal of nucleons with Fermi momentum distributions. However, their experimental values for the transverse velocity dispersions of the fragments seem about an order of magnitude less than those probed by pions obtained in the present experiment. Thus the oblateness of inclusive projectile-fragment velocity distributions cannot simply account for the oblateness of the π^- peaks. The transverse dispersion is clearly dependent on the impact parameter of the reaction when it is measured directly by projectile fragments, but is rather constant if it is observed through projectile-rapidity pions. It might be because pions are probing an earlier stage of reaction and dispersion of projectile fragments which are at much higher temperature. Further theoret-

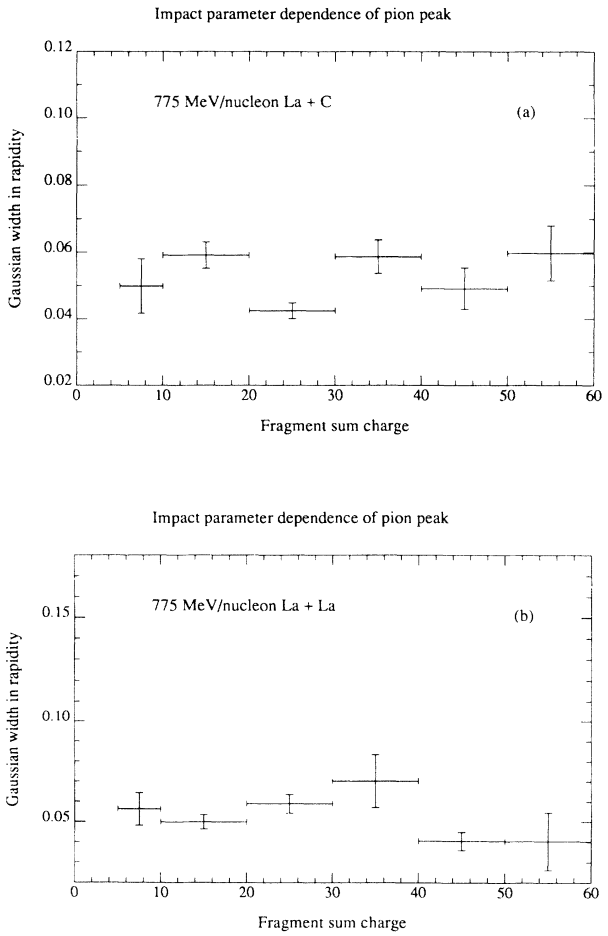

FIG. 7. Same as Fig. 6 except that the Gaussian width parameters in the rapidity are plotted as a function of rapidity. (a) La + C reaction, (b) La + La reaction.

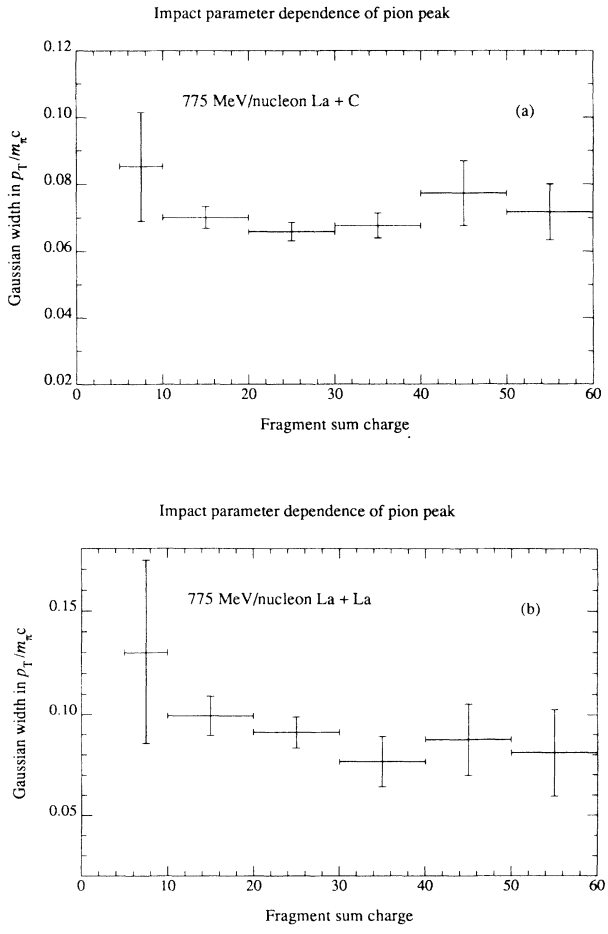

FIG. 8. Same as Fig. 7 except that fitted Gaussian width parameters in transverse momentum (units $m_\pi c$) are shown. (a) La + C reaction, (b) La + La reaction.

ical studies on the pion production and reabsorption by nonspherical projectile fragments will be needed.

V. SUMMARY

The pions emitted at forward angle were measured in coincidence with the projectile fragments in the La + C and La reactions at the incident energy of 775 MeV/nucleon. Three physical quantities were correlated with each other, namely, pion rapidity (y), pion transverse momentum ($p_T/m_\pi c$), and projectile fragment "sum charge." The center of the pion peak position showed clear downshifts in the longitudinal direction as sum charge decreased. We attribute the shifts to the increasing deceleration of the projectile fragments in the more central collisions, assuming that the pion peak tracks the projectile motion. In addition, the pion peak showed oblate distribution, widths of which in longitudinal and transverse direction are much broader than those measured by the fragment momentum dispersion. It might be because the pion probes an earlier stage of the reaction when the "temperature" of the system is higher.

ACKNOWLEDGMENTS

We thank Dr. D. Greiner, Dr. H. Crawford, Dr. P. Lindstrom, Dr. F. Bieser, Dr. C. McParland, and all the members of the HISS group of LBL for their warm assistance which made the present experiment possible. Thanks are also due to Prof. O. Chamberlain, Prof. H. Steiner, Prof. H. Pugh, and Prof. K. Sugimoto for continuous encouragement. Technical assistance by Mr. R. Fuzesy, Mr. Y. Matsuyama, and Mr. K. Omata is greatly appreciated, as is the valuable help of Dr. S. Y. Chu in the final preparation of figures and manuscript. We also are very much indebted to the Bevatron crew for their skilled operation of the accelerator. The research was supported under the INS (Institute for Nuclear Study, University of Tokyo) - LBL collaborative program of the Ministry of Education, Japan and the U.S. Department of Energy under Contract DE-AC03-76SF00098.

[1] W. Benenson, G. Bertsch, G. M. Crawley, E. Kashy, J. A. Nolen, Jr., H. Bowman, J. G. Ingersoll, J. O. Rasmussen, J. Sullivan, M. Koike, M. Sasao, J. Peter, and T. E. Ward, Phys. Rev. Lett. **43**, 683 (1979); **44**, 54(E) (1980).

[2] J. P. Sullivan, J. A. Bistirlich, H. R. Bowman, R. J. Bossingham, T. Buttke, K. M. Crowe, K. A. Frankel, C. J. Martoff, J. Miller, D. L. Murphy, J. O. Rasmussen, W. A. Zajc, O. Hashimoto, M. Koike, J. Peter, W. Benenson, G. M. Crawley, E. Kashy, and J. A. Nolen, Phys. Rev. C **25**, 1499 (1982).

[3] D. Lebrun, J. Chauvin, D. Rebreyend, G. Perrin, P. De Saintignon, P. Martin, M. Buenerd, C. Lebrun, J. F. Lecolley, Y. Cassagnou, J. Julien, and R. Legrain, Phys. Lett. B **223**, 139 (1989); D. Lebrun, J. Chauvin, J. Julien, C. Lebrun, J. F. Lecolley, G. Perrin, D. Rebreyend, and P. De Saintignon, Z. Phys. A **335**, 73 (1990).

[4] K. G. Libbrecht and S. E. Koonin, Phys. Rev. Lett. **43**, 1581 (1979).

[5] J. Cugnon and S. E. Koonin, Nucl. Phys. **A355**, 477 (1981).

[6] M. Gyulassy and S. K. Kauffmann, Nucl. Phys. **A362**, 503 (1981).

[7] H. M. A. Radi, J. O. Rasmussen, J. P. Sullivan, K. A. Frankel, and O. Hashimoto, Phys. Rev. C **25**, 1518 (1982).

[8] J. Engelage, M. E. Baumgartner, E. Beleal, B. Berman, F. Bieser, F. P. Brady, M. Bronson, J. B. Carroll, H. J. Crawford, I. Flores, D. E. Greiner, L. Greiner, O. Hashimoto, G. Igo, S. Kadota, P. N. Kirk, P. J. Lindstrom, C. McParland, S. Nagamiya, D. L. Olson, J. Porter, J. L. Romeo, C. L. Ruiz, T. J. M. Symons, I. Tanihata, R. Wada, M. L. Webb, J. Yamada, and H. Lee, Nucl. Instrum. Methods **A277**, 431 (1989).

[9] J. C. Alder, B. Gabioud, C. Joseph, J. F, Loude, N. Morel, A. Perrenoud, J. P. Perroud, M. T. Tran, B. Vaucher, E. Winkelmann, D. Renker, H. Schmitt, C. Zupancic, H. von Fellenberg, A. Frischknecht, F. Hoop, G. Strassner, and P. Truol, Nucl. Instrum. Methods. **160**, 93 (1979).

[10] S. Hayashi, Y. Miake, T. Nagae, S. Nagamiya, H. Hamagaki, O. Hashimoto, Y. Shida, I. Tanihata, K. Kimura, O. Yamakawa, T. Kobayashi, and X. X. Bai, Phys. Rev. C **38**, 1229 (1988).

[11] F. P. Brady, W. B. Christie, J. L. Romero, C. E. Tull, B. McEachern, M. L. Webb, J. C. Young, H. Crawford, D. E. Greiner, P. J. Lindstrom, and H. Sann, Phys. Rev. Lett. **60**, 1699 (1988); cf. C. E. Tull, Ph.D. thesis, U. C. Davis, LBL Report 29718 (1989) unpublished.

[12] J. Hubble, *et al.*, Z. Phys. A **340**, 263 (1991).